Short note

The Pliocene Xoconostle high sulfidation epithermal deposit in the Trans-Mexican Volcanic Belt: Preliminary study

El depósito epitermal de alta sulfuración pliocénico Xoconostle en la Faja Volcánica Trans-Mexicana: Estudio preliminar

Edith **Fuentes-Guzmán**[1,2,3], Antoni **Camprubí**[1,*], Janet **Gabites**[4], Eduardo **González-Partida**[5], Vanessa **Colás**[1]

[1] Instituto de Geología, Universidad Nacional Autónoma de México. Ciudad Universitaria, 04510 Coyoacán, CDMX, Mexico.

[2] Programa de Posgrado en Ciencias de la Tierra, Universidad Nacional Autónoma de México. Ciudad Universitaria, 04510 Coyoacán, CDMX, Mexico.

[3] Laboratorio Nacional de Geoquímica y Mineralogía (LANGEM). Ciudad Universitaria, 04510 Coyoacán, CDMX, Mexico.

[4] Pacific Centre for Isotopic and Geochemical Research, Department of Earth, Ocean and Atmospheric Sciences, University of British Columbia; Earth Sciences Building, 2207 Main Mall, Vancouver, British Columbia, V6T 1Z4, Canada.

[5] Centro de Geociencias, Universidad Nacional Autónoma de México. Boulevard Juriquilla 3001, 76230 Juriquilla, Querétaro, Mexico.

* Corresponding author: (A. Camprubí) *camprubi@comunidad.unam.mx*

How to cite this article:
Fuentes-Guzmán, E., Camprubí, A., Gabites, J., González-Partida, E., Colás, V., 2020, The Pliocene Xoconostle high sulfidation epithermal deposit in the Trans-Mexican Volcanic Belt: Preliminary study: Boletín de la Sociedad Geológica Mexicana, 72 (3), A260520. http://dx.doi.org/10.18268/BSGM2020v72n3a260520

Manuscript received: March 3, 2019
Corrected manuscript received: May 10, 2020
Manuscript accepted: May 25,2020

Peer Reviewing under the responsibility of Universidad Nacional Autónoma de México.

ABSTRACT

The Xoconostle prospect in northeastern Michoacán state, south-central Mexico, is constituted by high sulfidation epithermal breccias and stockworks with Au and Hg prospective anomalies. The mineralization is hosted by latest Miocene to Pliocene rocks grouped into the El Terrero ignimbrite and the Siete Cruces dome complex and a stock of intermediate composition and undetermined (Pliocene?) age. Two alunite samples from deep hypogene advanced argillic alteration assemblages within the deposit yielded $^{40}Ar/^{39}Ar$ ages at 5.57 ± 0.44 (Messinian) and 3.67 ± 0.20 Ma (Zanclean). Such ages are in good agreement with those of volcanic rocks at a semi-regional scale, especially those associated with the nearby Amealco caldera. Assuming that the formation of Xoconostle deposit could be genetically related to any of the eruptive units in this caldera, it would be associated with dacitic-andesitic rocks at ~4.7 Ma or with bimodal andesite-basalt volcanism at ~3.7 Ma, with which rhyolites at the southwest rim of the caldera (nearer to the epithermal deposit) are contemporaneous. The obtained ages are also in good agreement with those determined for the youngest stages in the evolution of the Trans-Mexican Volcanic Belt (TMVB). In addition, such ages compare well with those established for the E-W striking Morelia-Acambay normal fault zone (or Acambay graben). The occurrence of E-W structural features in the study area support their correlation with those in the Acambay graben. Although the metallogenesis of the TMVB needs further endeavours that contribute to its understanding, the Xoconostle prospect adds up to other dated magmatic-hydrothermal deposits that may collectively constitute a Pliocene metallogenic province whose inception was geologically circumscribed to this volcanic arc. However, this and its companion papers in this issue confirm the metallogenic potential of the TMVB in most of its stages of evolution, particularly in the late Miocene-Pliocene stage of acid and bimodal volcanism.

Keywords: Epithermal, high sulfidation, $^{40}Ar/^{39}Ar$ ages, alunite, Pliocene, Mexico, Trans-Mexican Volcanic Belt, regional metallogeny.

RESUMEN

El prospecto Xoconostle, al noreste del estado de Michoacán en el sur-centro de México, está constituido por brechas y stockworks epitermales de alta sulfuración que contienen anomalías prospectivas en Au y Hg. Este depósito está alojado por rocas del Mioceno terminal al Plioceno que se agrupan en la ignimbrita El Terrero y el complejo de domos Siete Cruces, además de un stock de composición intermedia y edad indeterminada (¿Plioceno?). Dos muestras de alunita procedentes de asociaciones de alteración argílica avanzada hipogénica profunda en el depósito arrojaron edades $^{40}Ar/^{39}Ar$ de 5.57 ± 0.44 (Messiniano) y 3.67 ± 0.20 Ma (Zancleano). Dichas edades son contemporáneas con las edades de rocas volcánicas a escala semi-regional, particularmente las asociadas a la cercana caldera de Amealco. Asumiendo que la formación del depósito de Xoconostle pudiera estar relacionada genéticamente con alguna de las unidades eruptivas que se encuentran en esta caldera, éste se asociaría con rocas dacíticas-andesíticas de ~4.7 Ma o bien con volcanismo bimodal andesítico-basáltico de ~3.7 Ma, con el cual son contemporáneas riolitas del extremo suroccidental del borde de la caldera (el más cercano al depósito epitermal). Las edades obtenidas también se corresponden bien, a escala regional, con las determinadas para las etapas más recientes en la evolución de la Faja Volcánica Trans-Mexicana (FVTM). Adicionalmente, dichas edades son congruentes con las determinadas para la zona de fallas normales E-W Morelia-Acambay (o graben de Acambay). La presencia de rasgos estructurales con orientación E-W en el área de estudio apoya la correlación de éstos con los del graben de Acambay. Aunque la metalogenia de la FVTM precisa de mayor esfuerzo para contribuir a su mejor comprensión, el prospecto Xoconostle se agrega al conjunto de otros depósitos magmático-hidrotermales ya fechados que pudieran constituir colectivamente una provincia metalogenética en el Plioceno cuyo origen haya estado circunscrito geológicamente al de este arco volcánico. Sin embargo, éste y los trabajos que lo acompañan en este número confirman el potencial metalogenético de la FVTM en la mayoría de sus etapas evolutivas, particularmente en la etapa de volcanismo ácido y bimodal del Mioceno tardío-Plioceno.

Palabras clave: Epitermal, alta sulfuración, edades $^{40}Ar/^{39}Ar$, alunita, Plioceno, México, Faja Volcánica Trans-Mexicana, metalogenia regional.

http://dx.doi.org/10.18268/BSGM2020v72n3a260520

1. Introduction

The metallogenic potential of the mid-Miocene to Recent Trans-Mexican Volcanic Belt (TMVB) and Miocene to Recent ore deposits in Mexico have been traditionally set aside in regional exploration endeavours and metallogenic overviews. However, advances in the last decades have begun to stress the importance of the Miocene to Recent metallogeny of Mexico, including the TMVB (Camprubí, 2009, 2013; Clark and Fitch, 2009; Poliquin, 2009; Jansen *et al.*, 2017; Camprubí *et al.*, 2019, 2020; Fuentes-Guzmán *et al.*, 2020). The mineralization in the Xoconostle prospect is associated with volcanic and hypabyssal rocks of the Michoacán-Guanajuato volcanic field (part of the TMVB), which range in age between the late Miocene and Holocene (Pasquarè *et al.*, 1988; Pérez-Orozco *et al.*, 2018). Such ages are consistent with the youngest regional metallogenetic episodes proposed by Camprubí (2009, 2013). These deposits were earlier described as Au-Ag-Hg hot spring-style epithermal low sulfidation ore bodies that were mined at a small scale for mercury (Arredondo *et al.*, 1989; Morales-Alvarado, 1996).

This paper aims to contribute to the characterization of the metallogeny of the TMVB, which is one of the youngest metallogenic provinces in the region. In this case, alunite from a deep hypogene advanced argillic assemblage is dated. This paper is circumscribed to a long-standing program that aims to understand the geochronological characterization of Mexican mineral deposits and the geologic events with which they are associated in time, space and genesis (Camprubí *et al.*, 2003, 2015, 2016a, 2016b, 2017, 2018, 2019, 2020; Farfán-Panamá *et al.*, 2015; Martínez-Reyes *et al.*, 2015; González-Jiménez *et al.*, 2017a, 2017b; Enríquez *et al.*, 2018; Fuentes-Guzmán *et al.*, 2020), to better constrain the metallogenic evolution of Mexico, as essayed by Camprubí (2009, 2013, 2017).

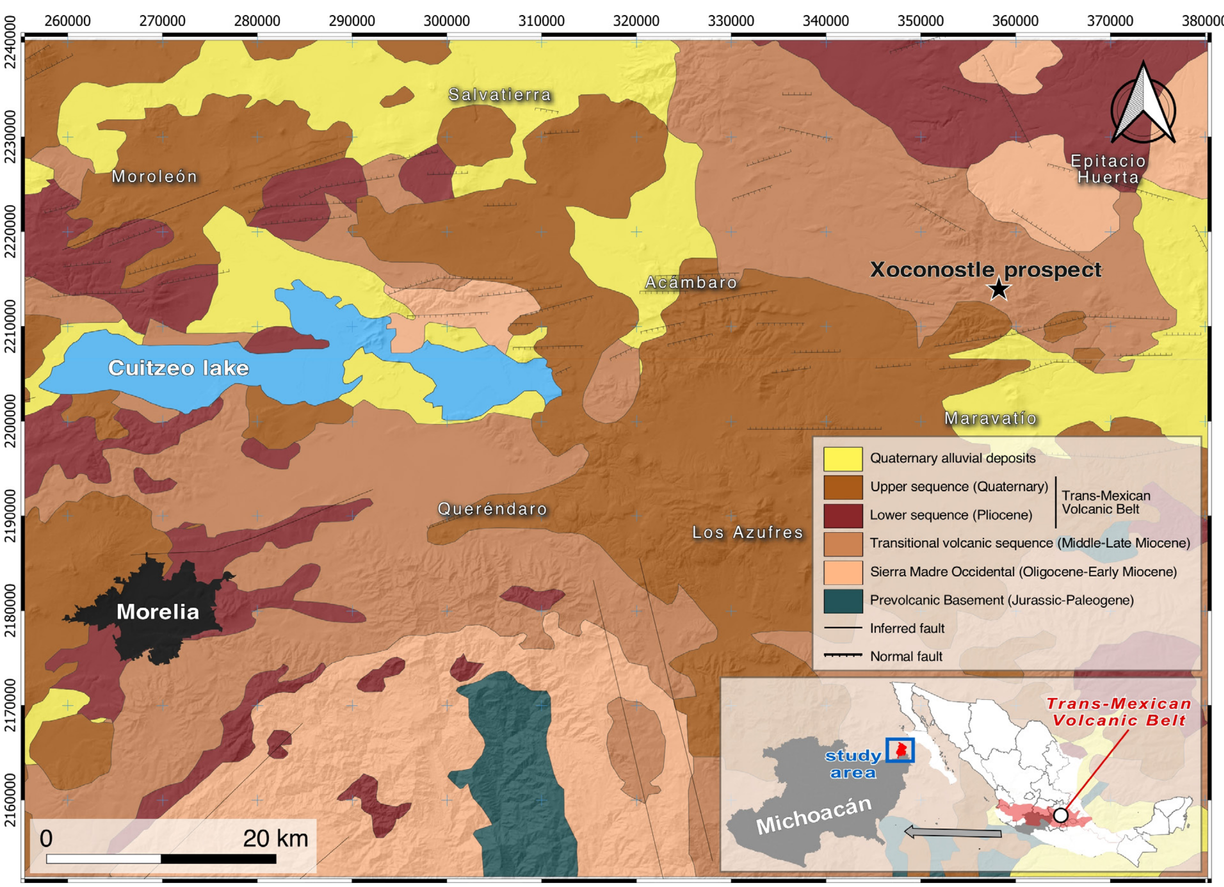

Figure 1 Regional geological map including the Xoconostle high sulfidation epithermal deposit, modified from Pasquarè *et al.* (1988).

http://dx.doi.org/10.18268/BSGM2020v72n3a260520

2. Geology

The Xoconostle epithermal deposit (Servicio Geológico Mexicano, 2002) is associated with the E-W regional-scale Morelia-Acambay normal fault zone (or Acambay graben; Martínez-Reyes and Nieto-Samaniego, 1990; Garduño-Monroy *et al.*, 2009; Pérez-Orozco *et al.*, 2018). The activity of this fault zone probably started at ~10 Ma as left-lateral faults (Garduño-Monroy *et al.*, 2009) followed by extensional displacement with the hanging walls tilted northwards due to listric faults (Israde-Alcántara and Garduño-Monroy, 1999).

During the Quaternary, these faults show normal displacements and a left-lateral strike slip component characterized by a left-lateral transtensive deformation (Suter *et al.*, 1992, 2001; Ego and Ansan, 2002). Some of the segments in the Morelia-Acambay normal fault zone show evidence for movement between the late Pleistocene and the Holocene (Langridge *et al.*, 2000; Suter *et al.*, 2001; Garduño-Monroy *et al.*, 2009, in Pérez-Orozco *et al.*, 2018). A noteworthy geological feature in the region is the Amealco caldera, northeast of the Xoconostle deposit.

In the study area, Pliocene to Holocene volcanic and subvolcanic rocks of the TMVB crop out. From older to younger, these rocks include: the El Terrero ignimbrite (andesitic-dacitic; 6.12 ± 0.60 Ma), the Siete Cruces dome complex (rhyolites; 5.45 ± 0.50 Ma), and the Amealco unit (basalts, andesites, and ash-fall deposits; ca. 3 Ma; Murillo-Muñetón and Torres-Vargas, 1987; Pasquarè *et al.*, 1988; Aguirre-Díaz and McDowell, 2000). Such units overlie Miocene volcanic rocks geologically circumscribed to the Sierra Madre Occidental, and late Miocene basalts and andesites constituiting the earliest manifestations of the TMVB (Pasquarè *et al.*, 1988). Pliocene ages were previously deduced for the Xoconostle deposit based on the age of the host dacitic and rhyolitic rocks of the El Terrero ignimbrite and the Siete Cruces dome complex (Camprubí, 2009, 2013). Locally, an intermediate stock was pervasively altered with advanced argillic assemblages (Morales-Alvarado, 1996), but no clear genetic relationship between this stock and the epithermal mineralization can be determined.

The epithermal ore bodies of the Xoconostle prospect (also known as San Antonio, or El Cinabrio) are located approximately at the 20°01'06"N and 100°20'42"W geographic coordinates, in the Epitacio Huerta municipality in the northeasternmost tip of the state of Michoacán in south-central Mexico (Figure 1).

These bodies consist of breccias (3 to 20 m wide, and undetermined vertical extent) predominantly cemented by massive aggregates and stockworks of silica minerals (chalcedony, opal, quartz, cristobalite and tridymite, determined by XRD), associated with three prominent alteration zones (Arredondo *et al.*, 1989; Prol-Ledesma, 1990; Morales-Alvarado, 1996) from inner to outer: (1) silicification, comprising quartz, opal, tridymite, cristobalite and anatase, grading into (2) advanced argillic zone, comprising kaolinite, alunite, quartz, chalcedony, and pyrite, up to ~400 m wide, and into (3) argillic zone including kaolinite, cristobalite, and quartz. Propylitic alteration including chlorite, epidote, illite, and calcite occurs farther from the ore bodies in isolated patches. The ore-bearing assemblages contain pyrite, sphalerite, hematite, cinnabar, auricupride [Cu_3Au] and supergene iron oxihydroxides within massive to crudely banded silica (quartz, opal and chalcedony) ore bodies (Prol-Ledesma, 1990; Morales-Alvarado, 1996). Despite its depiction in early works as a low sulfidation deposit, we consider, based on our studies, that the characteristics of the Xoconostle prospect are more compatible with a high sulfidation epithermal deposit. Exploration surveys indicate grades up to 3 ppm Au and up to 1.3 wt.% Hg in the mineralized area (Arredondo *et al.*, 1989; Morales-Alvarado, 1996). Induced polarization (IP) surveys allow determining prospective areas where breccias and stockworks were later found (Arredondo *et al.*, 1989). The microthermometric study of fluid inclusions in the Xoconostle deposit yielded temperatures of homogenization that range between 140° and 240 °C, and calculated salinities at ~0.1 wt.% NaCl equiv. (Prol-Ledesma, 1990).

http://dx.doi.org/10.18268/BSGM2020v72n3a260520

3. Methods and results

Two pure alunite mineral separates from outcropping epithermal alteration material from the Xoconostle prospect were dated by $^{40}Ar/^{39}Ar$ geochronology (Table 1). The analyzed samples correspond to alunite crystals separated from deep hypogene advanced argillic alteration assemblages adjacent to the main massive quartz ore body in the high sulfidation epithermal deposits. These samples were massive, not pulverulent, aggregates of white to slightly rose-hued fine-grained and euhedral to subhedral platy alunite crystals. Hence we classify the advanced argillic alteration assemblage to which this alunite belongs as deep hypogene (*e.g.*, Sillitoe, 1993, 2015).

The alunite samples were crushed in a ring mill, washed in distilled water and ethanol, and sieved when dry to -40+60 mesh. Appropriate mineral grains were picked out of the bulk fraction. The samples were wrapped in aluminum foil and stacked in an irradiation capsule with similar-aged samples and neutron flux monitors (Fish Canyon Tuff sanidine [FCs], 28.201 ± 0.046 Ma; Kuiper *et al.*, 2008). The samples were irradiated in October 2017 at the McMaster Nuclear Reactor in Hamilton, Ontario, in a shielded can for 6 MWH in the medium flux site 8E. Analyses (n = 39) of 13 neutron flux monitor positions produced errors of <0.5% in the J value. The samples were analyzed at the Noble Gas Laboratory, Pacific Centre for Isotopic and Geochemical Research (PCIGR) of The University of British Columbia in Vancouver, BC, Canada. The mineral separates were step-heated at incrementally higher powers in the defocused beam of a 10W CO_2 laser (New Wave Research MIR10) until fused. The gas evolved from each step was analyzed by a VG5400 mass spectrometer equipped with an ion-counting electron multiplier. All measurements were corrected for total system blank, mass spectrometer sensitivity, mass discrimination, radioactive decay during and subsequent to irradiation, as well as interfering Ar from atmospheric contamination and the irradiation of Ca, Cl and K. The isotope production ratios were: $(^{40}Ar/^{39}Ar)_K = 0.0005 \pm 0.00006$, $(^{37}Ar/^{39}Ar)_{Ca} = 1048 \pm 0.9$, $(^{36}Ar/^{39}Ar)_{Ca} = 0.3952 \pm 0.0004$, Ca/K = 1.83 ± 0.01($^{37}Ar_{Ca}/^{39}Ar_K$).

Details of the analyses, including plateau (spectrum) and inverse isochron plots, are presented in Table 1 and Figure 2. Initial data entry and calculations were carried out using the software ArArCalc (Koppers, 2002). The plateau and correlation ages were calculated using Isoplot v.3.09 (Ludwig, 2003). Errors are quoted at the 2-sigma (95% confidence) level and are propagated from all sources except mass spectrometer sensitivity and age of the flux monitor. The best statistically justified plateau and plateau age were picked based on the following criteria: (1) three or more contiguous steps comprising more than 60% of the ^{39}Ar, (2) probability of fit of the weighted mean age greater than 5%, (3) slope of the error-weighted line through the plateau ages equals zero at 5% confidence, (4) ages of the two outermost steps on a plateau are not significantly different from the weighted-mean plateau age (at 1.8σ six or more steps only), and (5) outermost two steps on either side of a plateau must not have nonzero slopes with the same sign (at 1.8σ nine or more steps only). The analyzed samples yielded, as best estimates, plateau ages at 5.57 ± 0.44 and 3.67 ± 0.20 Ma, that we interpret as the ages of deep hypogene hydrothermal alteration associated to the mineralization of the Xoconotle prospect (Figure 2).

4. Discussion and conclusions

As the host rocks to the Xoconostle high sulfidation epithermal deposits are the El Terrero ignimbrite (andesitic-dacitic; 6.12 ± 0.60 Ma; Pasquarè *et al.*, 1988) and the Siete Cruces dome complex (rhyolites; 5.45 ± 0.50 Ma; Pasquarè *et al.*, 1988), both $^{40}Ar/^{39}Ar$ alunite ages obtained in this study constitute a reasonable approximation to the age of the deposit, despite the ~2 Myr discrepancy between the 5.57 ± 0.44 Ma (Messinian,

http://dx.doi.org/10.18268/BSGM2020v72n3a260520

Table 1. $^{40}Ar/^{39}Ar$ determination dataset for two alunite samples from deep hypogene advanced argillic alteration assemblages in the Xoconostle high sulfidation epithermal deposit.

EH21 Alunite															
Laser	Isotope Ratios														
Power (%)	$^{40}Ar/^{39}Ar$	2σ	$^{36}Ar/^{39}Ar$	2σ	$^{39}Ar/^{40}Ar$	2σ	$^{36}Ar/^{40}Ar$	2σ	Rho	K/Ca	%^{40}Ar rad	f ^{39}Ar	$^{40}Ar^{*}/^{39}ArK$	Age	2σ
2.1	329.34	7.90	1.4950	0.0915	0.0030	0.0001	0.0045	0.0003	0.097	13.63	8.31	1.25	27.355	7.80	± 5.35
2.2	223.01	4.50	1.0208	0.0607	0.0045	0.0001	0.0046	0.0003	0.102	12.52	7.54	2.55	16.827	4.80	± 3.62
2.3	140.87	6.11	0.6059	0.0417	0.0071	0.0003	0.0043	0.0002	0.101	12.77	13.13	5.96	18.502	5.28	± 2.17
2.4	113.49	2.11	0.4665	0.0272	0.0088	0.0002	0.0041	0.0002	0.055	7.65	16.98	8.92	19.271	5.50	± 1.61
2.5	99.73	4.61	0.4043	0.0300	0.0100	0.0005	0.0041	0.0002	0.021	8.12	18.13	10.46	18.085	5.16	± 1.48
2.6	84.44	1.94	0.3157	0.0187	0.0118	0.0003	0.0037	0.0002	0.102	5.95	24.49	17.93	20.685	5.90	± 1.12
2.6	71.81	1.62	0.2551	0.0153	0.0139	0.0003	0.0036	0.0002	0.087	6.88	28.25	21.27	20.291	5.79	± 0.91
2.7	73.08	1.28	0.2699	0.0158	0.0137	0.0002	0.0037	0.0002	0.064	10.00	25.42	15.46	18.578	5.30	± 0.95
2.8	77.87	1.56	0.2882	0.0168	0.0128	0.0003	0.0037	0.0002	0.086	11.91	25.27	16.20	19.677	5.61	± 1.01

J = 0.00015610 ± 0.00000023 Volume ^{39}ArK = 0.400 x E-13 cm3 NPT

Integrated Date = 5.57 ± 0.44 Ma

Age = 5.57±0.44 Ma (2s, including J-error of .5%) MSWD = 0.27, probability = 0.98 100% of the ^{39}Ar steps 1 through 9

Inverse isochron (correlation age) results: Model 1 Solution (±95%-conf.) on 9 points

Age = 5.4±1.0 Ma Initial $^{40}Ar/^{36}Ar$ =202.5±9.3 MSWD = 0.34 Probability = 0.53

XOC-6 alunite															
Laser	Isotope Ratios														
Power (%)	$^{40}Ar/^{39}Ar$	2σ	$^{36}Ar/^{39}Ar$	2σ	$^{39}Ar/^{40}Ar$	2σ	$^{36}Ar/^{40}Ar$	2σ	Rho	K/Ca	%^{40}Ar rad	*f* ^{39}Ar	$^{40}Ar^{*}/^{39}ArK$	Age	2σ
2.00	56.13	17.02	0.17	0.07	0.02	0.005	0.0031	0.0009	0.111	5.68	7.94	0.01	4.459	30.89	± 108.87
2.30	10.75	0.15	0.035	0.0018	0.09	0.001	0.0033	0.0002	0.027	6.34	2.28	2.94	0.245	1.71	± 3.70
2.80	1.35	0.02	0.003	0.0001	0.75	0.011	0.0021	0.0001	0.048	20.56	37.96	47.41	0.511	3.57	± 0.28
3.10	1.41	0.02	0.003	0.0001	0.71	0.013	0.0021	0.0001	0.139	24.63	38.31	31.16	0.541	3.78	± 0.31
3.40	2.73	0.06	0.007	0.0004	0.37	0.008	0.0026	0.0001	0.208	22.61	21.35	6.36	0.583	4.07	± 0.82
3.90	13.37	0.20	0.043	0.0022	0.07	0.001	0.0032	0.0002	0.029	12.94	4.01	4.18	0.537	3.75	± 4.51
4.40	13.93	0.21	0.046	0.0022	0.07	0.001	0.0033	0.0002	0.062	14.65	1.88	4.26	0.261	1.82	± 4.52
4.80	16.47	0.26	0.054	0.0027	0.06	0.001	0.0033	0.0002	0.063	11.73	1.28	3.69	0.211	1.47	± 5.56

J = 0.00381690 ± 0.00000573 Volume ^{39}ArK = 2.515 x E-13 cm3 NPT

Integrated Date = 3.67 ± 0.20 Ma

Plateau age = 3.67 ± 0.20 Ma (2s, including J-error of .2%) MSWD = 0.65, probability=0.71 Includes 100% of the ^{39}Ar steps 1 through 8

Inverse isochron (correlation age) results, plateau steps: Model 1 Solution (±95%-conf.) on 8 points

Age = 3.70 ± 0.26 Ma Initial $^{40}Ar/^{36}Ar$ =295.1 ± 7.4 MSWD = 0.62 Probability = 0.71

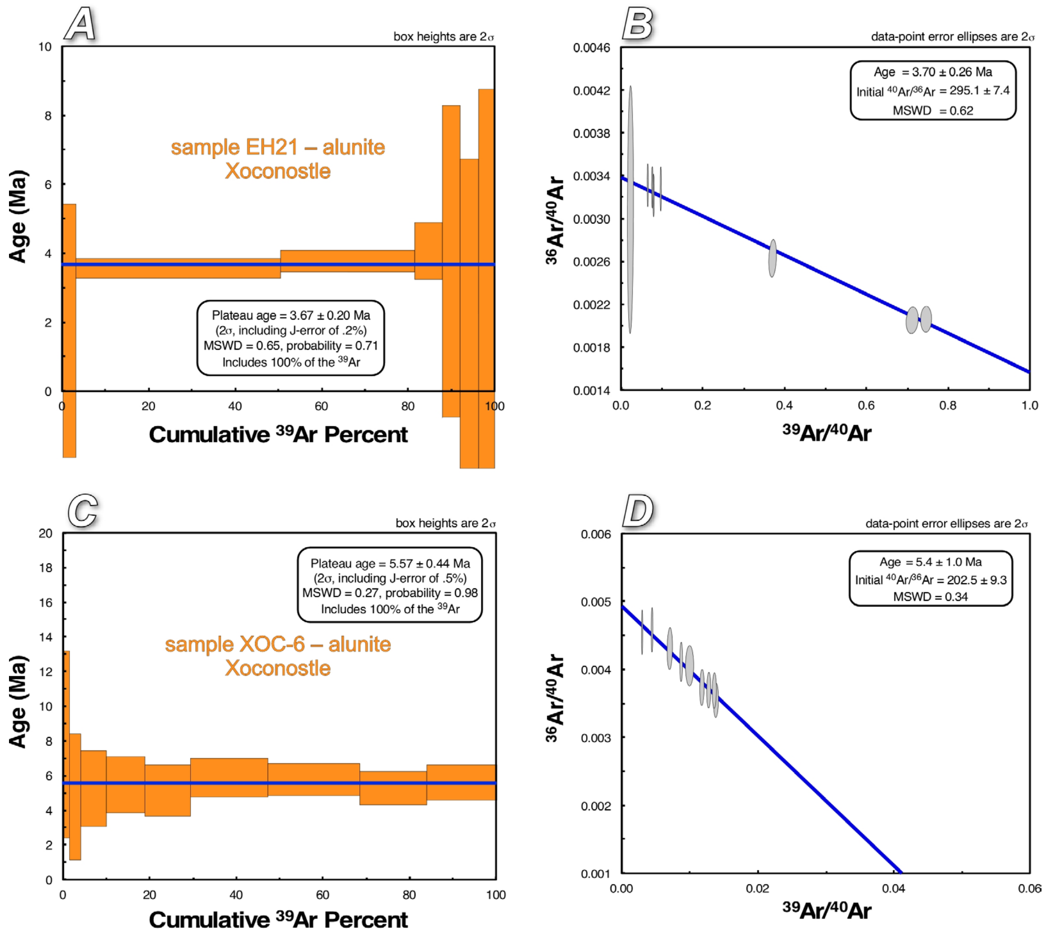

Figure 2 $^{40}Ar/^{39}Ar$ age plateau and inverse isochron diagrams for two dated alunite samples from deep hypogene advanced argillic alteration assemblages in the Xoconostle deposit.

latest Miocene) and the 3.67 ± 0.20 Ma (Zanclean, early Pliocene) ages (Figure 3). In high sulfidation epithermal deposits, their genetically associated magmatic rocks and the subsequent hydrothermal activity that generated the deposits are expected to span a short period of time of about a few kyr (*e.g.*, Arribas *et al.*, 1995; Jansen *et al.*, 2017). Also, the Amealco caldera, whose rim is located ~15 km to the northeast of the Xoconostle deposit, begun its activity at ~4.7 Ma with trachyandesites and trachydacites (Aguirre-Díaz and McDowell, 2000; Figure 3).

Therefore, even the 5.57 ± 0.44 Ma age could account for the formation of the deposit considering its standard deviation. In case the undated intermediate stock partially hosting the deposit (Morales-Alvarado, 1996) were younger than the 5.45 Ma dome complex, the likeliest age for the mineralization would be Zanclean, not Messinian. Among several episodes in its evolution since its inception, the Amealco caldera produced bimodal andesite-basalt volcanism at ~3.7 Ma, during an episode that also produced rhyolitic domes in its southwest rim (Aguirre-Díaz and McDowell, 2000; Figure 3). Such age would agree with subsequent hydrothermal activity at 3.67 ± 0.20 Ma in the Xoconostle deposit (Figure 3). Despite the geological likelihood of both ages in this study, to the present reckoning it would be premature to favoring one above the other (or not, thus implying hydrothermal activity for over 2 Myr), and further research would be instrumental for such decision.

The Morelia-Acambay normal fault zone (or Acambay graben) ranges in age between 4.7 and

http://dx.doi.org/10.18268/BSGM2020v72n3a260520

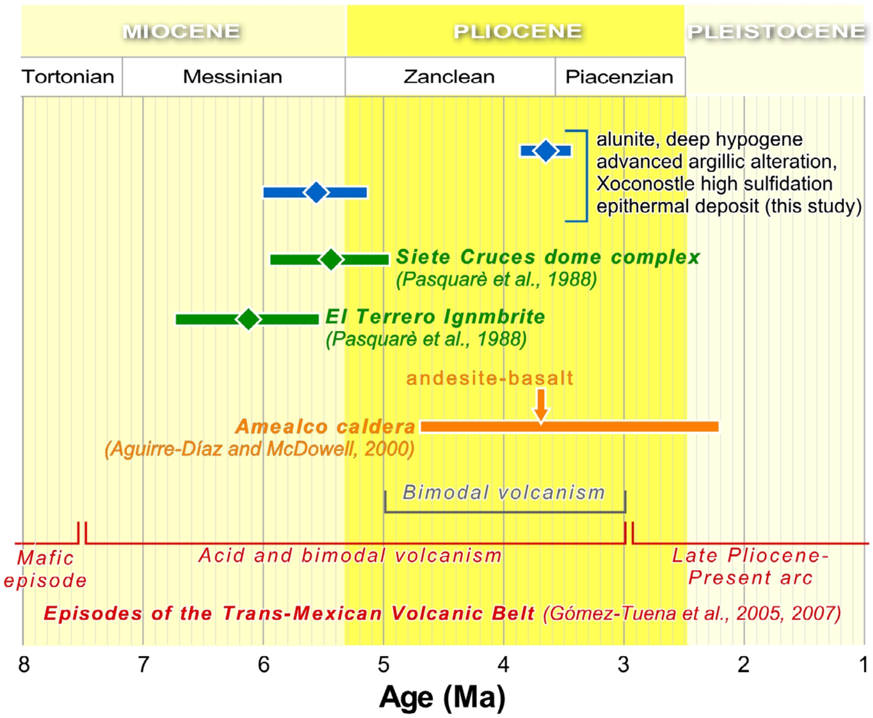

Figure 3 Summary of alunite ages in this study along with available ages for volcanism with which the Xoconostle deposit is more likely to be associated within the Trans-Mexican Volcanic Belt (TMVB).

2.2 Ma (Martínez-Reyes and Nieto-Samaniego, 1990; Aguirre-Díaz and McDowell, 2000; Aguirre-Díaz *et al.*, 2000; Garduño-Monroy *et al.*, 2009; Pérez-Orozco *et al.*, 2018), and the formation of the Xoconostle epithermal deposit is circumscribed to its characteristically E-W structural features (Servicio Geológico Mexicano, 2002). In that case, a Zanclean age for this deposit would fit better the known age constraints for regional geological features. The obtained ages in this study also compare well with the third stage of evolution of the Trans-Mexican Volcanic Belt (TMVB) of Gómez-Tuena *et al.* (2005, 2007), which is characterized by acid and bimodal volcanism, and predate the Late Pliocene-Present arc in the TMVB (Figure 3).

Setting aside the above considerations, the Xoconostle deposit is firmly circumscribed to the youngest manifestations of magmatism in the TMVB, and adds up to other magmatic-hydrothermal deposits in this geological province (Camprubí, 2009, 2013; Poliquin, 2009; Camprubí *et al.*, 2020; Fuentes-Guzmán *et al.*, 2020), confirming its significant metallogenic potential. Besides Xoconostle, at least another high sulfidation epithermal deposit occurs in the TMVB: the Caballo Blanco deposit in Veracruz, with possible late Miocene to Pliocene age (Cuttle and Giroux, 2017). A relatively small number of low sulfidation epithermal deposits in the eastern half of the TMVB has also been dated late Miocene to Pliocene in age (Poliquin, 2009; Camprubí *et al.*, 2020). Among them, it is worth noting the Ixtacamaxtitlán deposit in Puebla. As mentioned by Camprubí *et al.* (2020) and Fuentes-Guzmán *et al.* (2020), the TMVB contains one of the youngest metallogenic provinces in Mexico. Beyond the possibility of finding early Miocene magmatic-hydrothermal deposits in the TMVB (Camprubí, 2013; Fuentes-Guzmán *et al.*, 2020), this study, along with those of Poliquin (2009) and Camprubí *et al.* (2020) emphasizes the occurrence of late Miocene to Pliocene deposits in the region. Each group of deposits would be associated with the first and third stages in the magmatic evolution of the TMVB, according to Gómez-Tuena *et al.* (2005, 2007), which enhance its metallogenic potential. Also, recent magmatism originated several geothermal fields associated with the fourth stage of the TMVB, like the Pathé–Yexthó in Hidalgo and Querétaro, Los Azufres in Michoacán, or Acoculco in Puebla and Hidalgo (Camprubí, 2013, and references therein; Sosa-Ceballos *et al.*, 2018).

Acknowledgements

This paper is part of the first author's PhD thesis. E.F.G. acknowledges the support of CONACyT through a PhD grant and the permission granted by the Instituto de Geología UNAM to carry on with her thesis while being a part of its academic staff. Funding for this work was provided by CONACyT through research grant 155662 to A.C. and CONACyT-SENER pt. 4.1 Gemex-EU to E.G.P. Additional funding was provided by the Instituto de Geología UNAM, and the Centro de Geociencias UNAM through personal allocations. Rodrigo Delgado Sánchez is thanked for his assistance with Figure 1. Lisard Torró, Joaquín Proenza and Carl Nelson, the handling editors of this special issue, are especially thanked for their help and critical comments.

References

Aguirre-Díaz, G.J., McDowell, F.W., 2000, Volcanic evolution of the Amealco caldera, central Mexico, in Delgado-Granados, H., Aguirre-Díaz, G., Stock, J.M. (eds.), Cenozoic tectonics and volcanism of Mexico: Special Paper of the Geological Society of America, 334, 189-193. https://doi.org/10.1130/0-8137-2334-5.179

Aguirre-Díaz, G.J., Urrrutia-Fucugauchi, J., Soler-Arechalde, A.M., McDowell, F.W., 2000, Stratigraphy, K-Ar ages, and magnetostratigraphy of the Acambay graben, central Mexican Volcanic Belt, in Delgado-Granados, H., Aguirre-Díaz, G., Stock, J.M. (eds.), Cenozoic tectonics and volcanism of Mexico: Special Paper of the Geological Society of America, 334, 167-178. https://doi.org/10.1130/0-8137-2334-5.167

Arredondo, F., Flores, R., Muñoz, F., 1989, Evaluación geológica preliminary del prospecto "El Xoconostle", mpio. Epitacio Huerta, Mich.: unpublished report, Minas de San Luis, S.A. de C.V., Gerencia de Exploración Zona Sur, 20 p.

Arribas, A., Hedenquist, J.W., Itaya, T., Okada, T., Concepcion, R.A., Garcia Jr., J.S., 1995, Contemporaneous formation of adjacent porphyry and epithermal Cu-Au deposits over 300 ka in northern Luzon, Philippines: Geology, 23, 337-340. https://doi.org/10.1130/0091-7613(1995)023<0337:CFOAPA>2.3.CO;2

Camprubí, A., 2009, Major metallogenic provinces and epochs of Mexico: SGA News, 25, 1-21. https://e-sga.org/fileadmin/sga/newsletter/news25/SGANews25.pdf

Camprubí, A., 2013, Tectonic and metallogenic history of Mexico, in Colpron, M., Bissig, T., Rusk, B.G., Thompson, J.F.H., (eds.), Tectonics, metallogeny, and discovery: the North American Cordillera and similar accretionary settings: Littleton, Colorado, USA, Society of Economic Geologists. Society of Economic Geologists Special Publication, 17, 201-243. https://doi.org/10.5382/SP.17.06

Camprubí, A., 2017, The metallogenic evolution in Mexico during the Mesozoic, and its bearing in the Cordillera of Western North America. Ore Geology Reviews, 81, 1193-1214. https://doi.org/10.1016/j.oregeorev.2015.11.007

Camprubí, A., Ferrari, L., Cosca, M.A., Cardellach, E., Canals, À., 2003, Ages of epithermal deposits in Mexico: Regional significance and links with the evolution of Tertiary volcanism: Economic Geology, 98, 1029-1037. http://dx.doi.org/10.2113/gsecongeo.98.5.1029

Camprubí, A., González-Partida, E., Valencia, V.A., Barra, F., 2015, Geochronology of Mexican mineral deposits. I: the San Martín polymetallic skarn, Zacatecas: Boletín de la Sociedad Geológica Mexicana, 67, 119-122. https://dx.doi.org/10.18268/BSGM2015v67n1a10

Camprubí, A., Albinson, T., Iriondo, A., 2016a, Geochronology of Mexican mineral deposits. V: the Peñón Blanco epithermal deposit, Durango: Boletín de la Sociedad Geológica Mexicana, 68, 365-370. https://dx.doi.org/10.18268/BSGM2016v68n2a13

Camprubí, A., Iriondo, A., Martínez-López, M., Ramos-Rosique, A., 2016b, Geochronology of Mexican mineral deposits. IV: the Cinco Minas epithermal deposit, Jalisco: Boletín de la Sociedad Geológica Mexicana, 68, 357-364. https://dx.doi.org/10.18268/BSGM2016v68n2a12

Camprubí, A., González-Partida, E., Alfonso, P., López-Martínez, M., Iriondo, A., Cienfuegos-Alvarado, E., Gutiérrez-Armendáriz, E., Morales-Puente, P., Canet, C., González-Ruiz, L., 2017, The Late Cretaceous Guaynopa IOCG and Guaynopita porphyry copper deposits, Chihuahua, Mexico. Ore Geology Reviews, 81, 1096-1112. https://doi.org/10.1016/j.oregeorev.2016.01.006

Camprubí, A., Centeno-García, E., Tolson, G., Iriondo, A., Ortega, B., Bolaños, D., Abdullin, F., Portugal-Reyna, J.L., Ramos-Arias, M.A., 2018, Geochronology of Mexican mineral deposits. VII: the Peña Colorada magmatic-hydrothermal iron oxide deposit (IOCG "clan"), Colima: Boletín de la Sociedad Geológica Mexicana, 70, 633-674. https://dx.doi.org/10.18268/BSGM2018v70n3a4

Camprubí, A., Cabrera-Roa, M.A., González-Partida, E., Martínez-López, M., 2019, Geochronology of Mexican mineral deposits. VIII: the Zacatepec polymetallic skarn, Oaxaca: Boletín de la Sociedad Geológica Mexicana, 71, 207-218. https://dx.doi.org/10.18268/BSGM2019v71n1a11

Camprubí, A., Fuentes-Guzmán, E., Ortega-Larrocea, P., Colín-García, M., Gabites, J., Auqué, L.F., Colás, V., González-Partida, E., 2020, The Pliocene Ixtacamaxtitlán low sulfidation epithermal deposit (Puebla, Mexico): A case of fossil fungi consortia in a steam-heated environment: Boletín de la Sociedad Geológica Mexicana, 72(3), A140420.http://dx.doi.org/10.18268/BSGM2020v72n3a140420

Clark, K.F., Fitch, D.C., 2009, Evolución de depositos metalicos en tiempo y espacio en Mexico, in Clark, K.F., Salas-Pizá, G., Cubillas-Estrada, R., eds., Geología Económica de México, II Edición: Pachuca, Hidalgo, Servicio Geológico Mexicano, 62-133

Cuttle, J., Giroux, G., 2017, Technical report – Caballo Blanco project. Resource update – La Paila zone: Vancouver, British Columbia, Canada, Candelaria Mining Corporation, 78 p. https://www.candelariamining.com%2Fimages%2FCAND-Caballo-Blanco-Technical-Report-20Apr17pdf&usg=AOvVaw19xSAUpd0Z3t3erm6UoFnt

Ego, F., Ansan, V., 2002, Why is the central Trans-Mexican volcanic belt (102–99 W) in transtensive deformation?: Tectonophysics 359 (1), 189–208. https://doi.org/10.1016/S0040-1951(02)00511-5

Enríquez, E., Iriondo, A., Camprubí, A., 2018, Geochronology of Mexican mineral deposits. VI: the Tayoltita low-sulfidation epithermal district, Durango and Sinaloa: Boletín de la Sociedad Geológica Mexicana, 70, 531-547. https://dx.doi.org/10.18268/BSGM2018v70n2a13

Farfán-Panamá, J.L., Camprubí, A., González-Partida, E., Iriondo, A., González-Torres, E.A., 2015, Geochronology of Mexican mineral deposits. III: the Taxco epithermal deposit, Guerrero: Boletín de la Sociedad Geológica Mexicana, 67, 357-366. https://dx.doi.org/10.18268/BSGM2015v67n2a16

Fuentes-Guzmán, E., González-Partida, E., Camprubí, A., Hernández-Avilés, G., Gabites, J., Iriondo, A., Ruggieri, G., López-Martínez, M., 2020, The Miocene

Tatatila–Las Minas IOCG skarn deposits (Veracruz) as a result of adakitic magmatism in the Trans-Mexican Volcanic Belt: Boletín de la Sociedad Geológica Mexicana, 72 (3), A110520.http://dx.doi.org/10.18268/BSGM2020v72n3a110520

Garduño-Monroy, V.H., Pérez-Lopez, R., Israde-Alcantara, I., Rodríguez-Pascua, M.A., Szynkaruk, E., Hernández-Madrigal, V.M., García-Estrada, G., 2009, Paleoseismology of the southwestern Morelia-Acambay fault system, central Mexico: Geofísica Internacional, 48 (3), 319-335. http://ojs.geofisica.unam.mx/ojs6/index.php/RGI/article/view/29

Gómez-Tuena, A., Orozco-Esquivel, M.T., Ferrari, L., 2005, Petrogénesis ígnea de la Faja Volcánica Transmexicana: Boletín de la Sociedad Geológica Mexicana, 57, 227-283. http://dx.doi.org/10.18268/BSGM2005v57n3a2

Gómez-Tuena, A., Orozco-Esquivel, M.T., Ferrari, L., 2007, Igneous petrogenesis of the Trans-Mexican Volcanic Belt, in Alaniz-Álvarez, S.A., Nieto-Samaniego, Á.F., eds., Geology of México: Celebrating the centenary of the Geological Society of México: Boulder, Colorado, USA, The Geological Society of America. Geological Society of America Special Paper, 422, 129-182. https://doi.org/10.1130/2007.2422(05)

González-Jiménez, J.M., Camprubí, A., Colás, V., Griffin, W.L., Proenza, J.A., Belousova, E., Centeno-García E., O'Reilly, S.Y., Talavera, C., Farré-de-Pablo, J., Satsukawa, T., 2017a, The recycling of chromitites in ophiolites from southwestern North America: Lithos, 294-295, 53-72. https://doi.org/10.1016/j.lithos.2017.09.020

González-Jiménez, J.M., Proenza, J.A., Martini, M., Camprubí, A., Griffin, W.L., O'Reilly, S.Y., Pearson, N.J., 2017b, Deposits associated with ultramafic-mafic complexes in Mexico: the Loma Baya case: Ore Geology Reviews, 81, 1053-1065. https://doi.org/10.1016/j.oregeorev.2015.05.014

Israde-Alcántara, I., Garduño-Monroy, V.H., 1999, Lacustrine record in a volcanic intra-arc setting: the evolution of the Late Neogene Cuitzeo basin system (Central-western Mexico, Michoacán): Palaeogeography, Palaeoclimatology, Palaeoecology, 151 (1), 209-227. https://doi.org/10.1016/S0031-0182(99)00024-3

Jansen, N.H., Gemmell, J.B., Chang, Z., Cooke, D.R., Jourdan, F., Creaser, R.A., Hollings, P., 2017, Geology and genesis of the Cerro la Mina porphyry-high sulfidation Au (Cu-Mo) prospect, Mexico: Economic Geology, 112, 799-827. https://dx.doi.org/10.2113/econgeo.112.4.799

Koppers, A.P., 2002, ArArCALC – software for $^{40}Ar/^{39}Ar$ age calculations: Computers and Geosciences, 28, 605-619. https://doi.org/10.1016/S0098-3004(01)00095-4

Kuiper, K.F., Deino, A, Hilgen, F.J., Krijgsman, W., Renne, P.R., Wijbrans, J.R., 2008, Synchronizing rock clocks of Earth history: Science, 320, 500. https://doi.org/10.1126/science.1154339

Langridge, R.M., Weldon, R.J. II, Moya, J.C., Suárez, G., 2000, Paleoseismology of the 1912 Acambay earthquake and the Acambay-Tixmadejé fault, Trans-Mexican Volcanic Belt: Journal of Geophysical Research: Solid Earth, 105(B2), 3019-3037.

Ludwig, K.R., 2003, Isoplot 3.09 A Geochronological Toolkit for Microsoft Excel: Berkeley Geochronology Center, Special Publication, 4.

Martínez-Reyes, A., Nieto-Samaniego, A.F., 1990, Efectos geológicos de la tectónica reciente en la parte central de México: Revista Mexicana de Ciencias Geológicas, 9 (1), 33-50. http://rmcg.geociencias.unam.mx/index.php/rmcg/article/view/1282/1086

Martínez-Reyes, J.J., Camprubí, A., Uysal, I.T., Iriondo, A., González-Partida, E., 2015, Geochronology of Mexican mineral deposits. II: Veta Madre and Sierra epithermal vein systems, Guanajuato district: Boletín de la Sociedad Geológica Mexicana, 67, 349-355. https://dx.doi.org/10.18268/BSGM2015v67n2a15

Morales-Alvarado, M., 1996, Zoneamiento de la alteración hidrotermal en el prospecto minero El Xoconostle, Michoacán: Mexico City, Universidad Nacional Autónoma de México, unpublished MSc thesis, 59 p.

Murillo-Muñetón, G., Torres-Vargas, R., 1987, Mapa petrogenético y radiométrico de la República Mexicana: Instituto Mexicano del Petróleo, Subdirección de Tecnología de Exploración, informe del proyecto C-2010, 78 p., unpublished.

Pasquarè, G., Ferrari, L., Tibaldi, A., Garduño, V.H., Vezzoli, L., 1988, Geology of the central sector of Mexican volcanic belt, states of Guanajuato and Michoacán: Geological Society of America, Map and Chart Series, MCH 072, 20 p.

Pérez-Orozco, J.D., Sosa-Ceballos, G., Garduño-Monroy, V.H., Ramón Avellán, D., 2018, Felsic-intermediate magmatism and brittle deformation in Sierra del Tzirate (Michoacán- Guanajuato Volcanic Field): Journal of South American Earth Sciences, 85, 81-95. https://doi.org/10.1016/j.jsames.2018.04.021

Poliquin, M.J., 2009, Geology, geochemistry and age of intrusion-related mineralisation in Eastern Mexico: Exeter, U.K., University of Exeter, unpublished PhD dissertation, 398 p. http://hdl.handle.net/10036/108354

Prol-Ledesma, R.M., 1990, Prospecto minero Xoconostle: reporte preliminar: Comunicaciones Técnicas del Instituto de Geofísica, Serie Investigación, 117, 26 p.

Servicio Geológico Mexicano, 2002, Carta de dominios metalogenéticos, Querétaro F14-10, 1:250,000: Pachuca, Hidalgo, Mexico, Servicio Geológico Mexicano. https://mapserver.sgm.gob.mx/Cartas_Online/tematicas/F14-10_meta.pdf

Sillitoe, R.H., 1993, Epithermal models: genetic types, geometrical controls and shallow features, in Kirkham, R.V., Sinclair, W.D., Thorpe, R.I., Duke, J.M. (eds.), Mineral Deposit Modeling: Geological Association of Canada Special Paper, 40, 403-417.

Sillitoe, R.H., 2015, Epithermal paleosurfaces: Mineralium Deposita, 50, 767-793. https://doi.org/10.1007/s00126-015-0614-z

Sosa-Ceballos, G., Macías, J.L., Avellán, D.R., Salazar-Hermenegildo, N., Boijseauneau-López, M.E., Pérez-Orozco, J.D., 2018, The Acoculco Caldera Complex magmas: Genesis, evolution and relation with the Acoculco geothermal system: Journal of Volcanology and Geothermal Research, 358, 288-306. https://doi.org/10.1016/j.jvolgeores.2018.06.002

Suter, M., Quintero, O., Johnson, C.A., 1992, Active faults and state of stress in the central part of the Trans-Mexican volcanic belt. The Venta del Bravo Fault: Journal of Geophysical Research, 97, 11983-11994.

Suter, M., López Martínez, M., Quintero Legorreta, O., Carrillo Martínez, M., 2001, Quaternary intra-arc extension in the central Trans-Mexican volcanic belt: Geological Society of America Bulletin, 113 (6), 693-703. https://doi.org/10.1130/0016-7606(2001)113<0693:QIAEIT>2.0.CO;2